Probing for Leptonic Signatures from GRB030329 with AMANDA-II

Michael Stamatikos

University of Wisconsin, Madison

Department of Physics

michael.stamatikos@icecube.wisc.edu

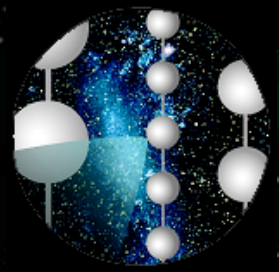

TeV Particle Astrophysics Workshop 2005

Fermi National Laboratory, Batavia IL

July 14, 2005

Talk Overview

I. **Introduction & Motivation:**

A. GRBs: Electromagnetic observables.
B. Fireball phenomenology & the GRB-neutrino connection.
C. GRB030329: a case study.

II. **Neutrino Astronomy & AMANDA-II:**

A. Flux models and detector response.
B. Optimization methods.

III. **Results:**

A. Neutrino flux upper limits for various models.
B. Comparison with other authors.

IV. **Conclusions & Future Outlook:**

A. Implications for correlative leptonic-GRB searches.

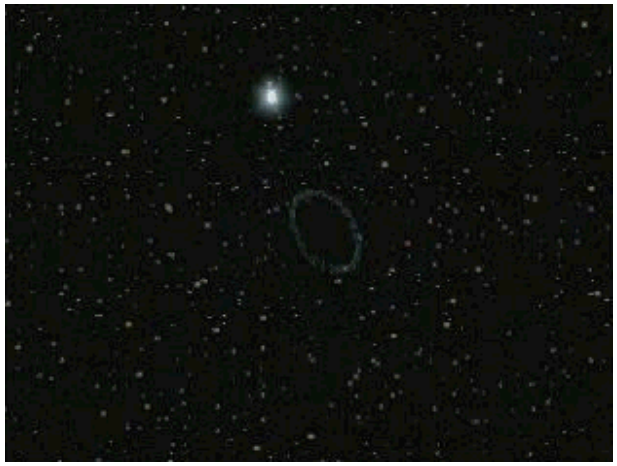

- Gamma-ray bursts (GRBs), discovered in the early 1970's by Vela satellites, are isotropically distributed transients of ~ keV - ~ 20 GeV radiation lasting for ~ 0.01 - ~ 1000 seconds.
- The Burst and Transient Source Experiment (BATSE) triggered over 2700 GRBs from 1993-2000, averaging about 1 GRB/day @ ~2/3 sky coverage.
- Progenitor models include compact binary mergers and the collapse of massive stars.
- The standard model of GRBs is characterized by the fireball phenomenology.
- GRB030329, detected by HETE-II, was a watershed transient, clinching the connection between GRBs and Type Ic SN. Due to rapid response via the GRB Coordinate Network

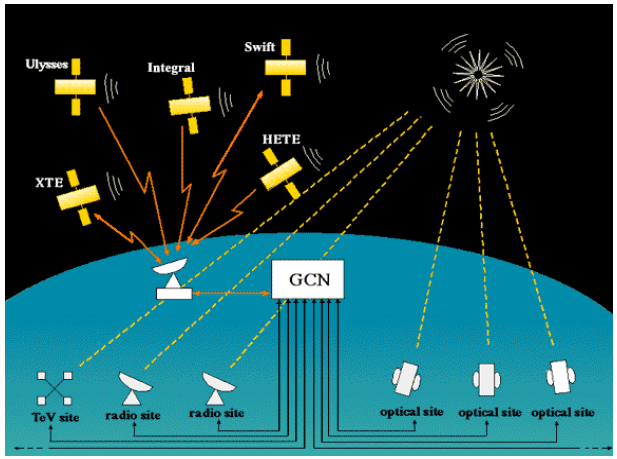

Gamma-Ray Bursts (GRBs): Prompt Emission

- GRBs are unique, varying from burst to burst and class to class (short, long, X-ray rich, non-triggered).
- Super-Eddington luminosities imply relativistic expansion.
- Millisecond temporal variability implies compact objects $R \leq 2\Gamma^2 c\Delta t$.
- Compactness problem resolved via $\sim 100 \leq \Gamma_{Bulk} \leq \sim 1000$, ensuring transparent optical depth to observed γ-ray photons, i.e. $\tau_{\gamma\gamma} \leq 1$.

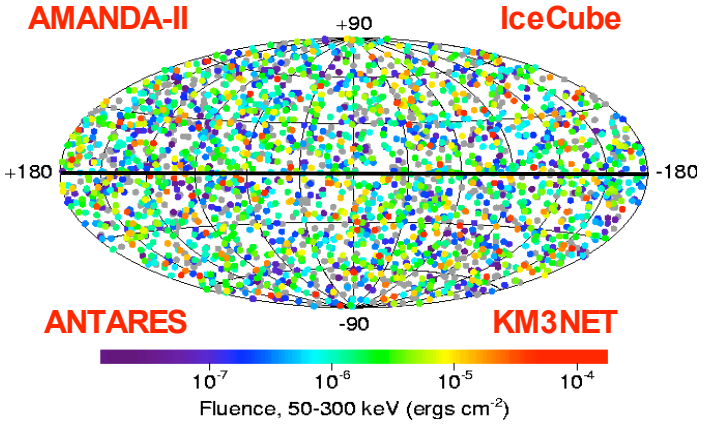

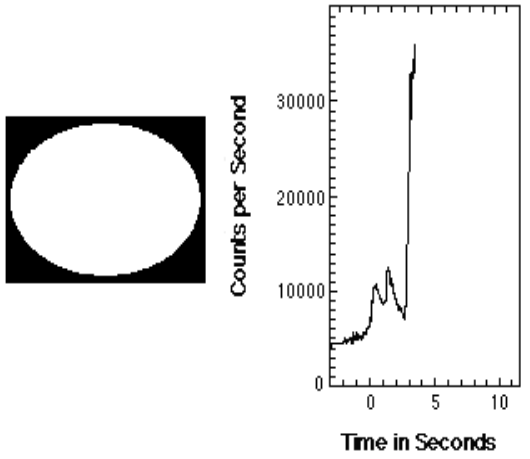

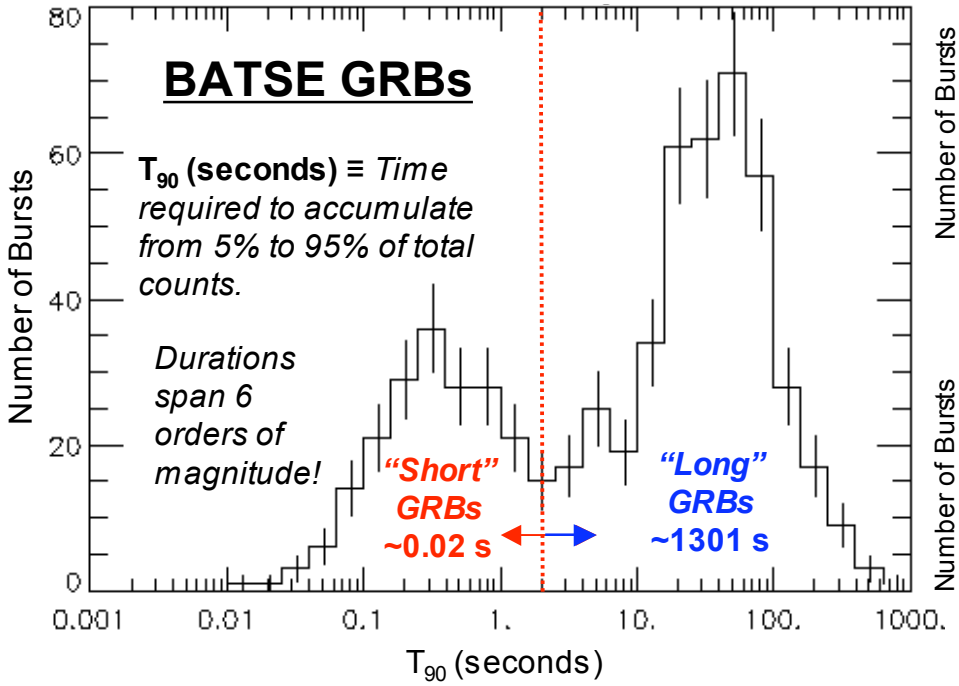

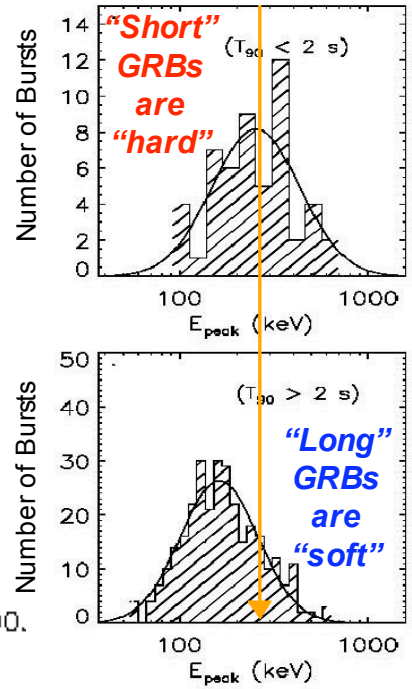

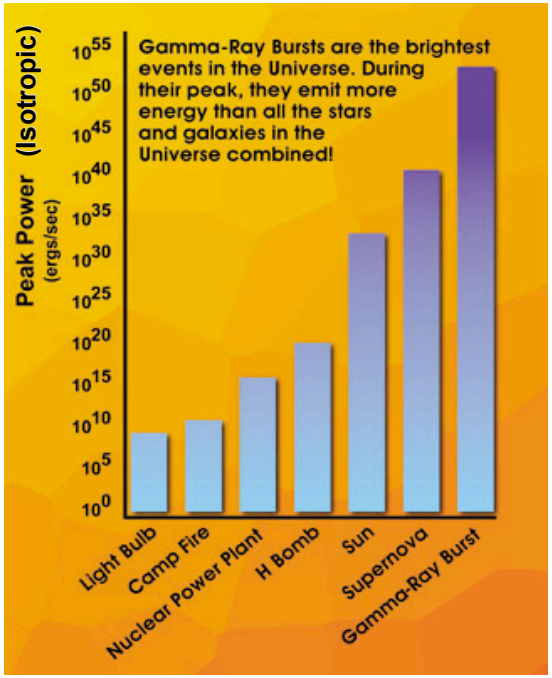

GRBs: Multi-Wavelength EM Afterglows

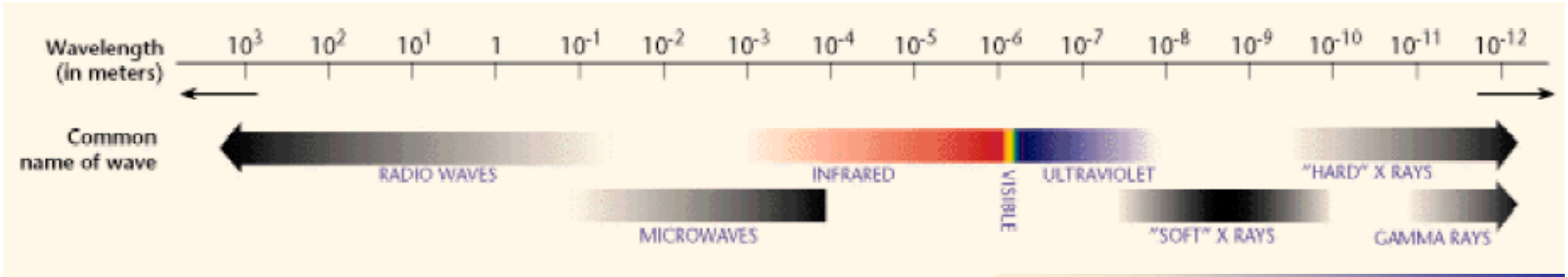

Prompt
Afterglow

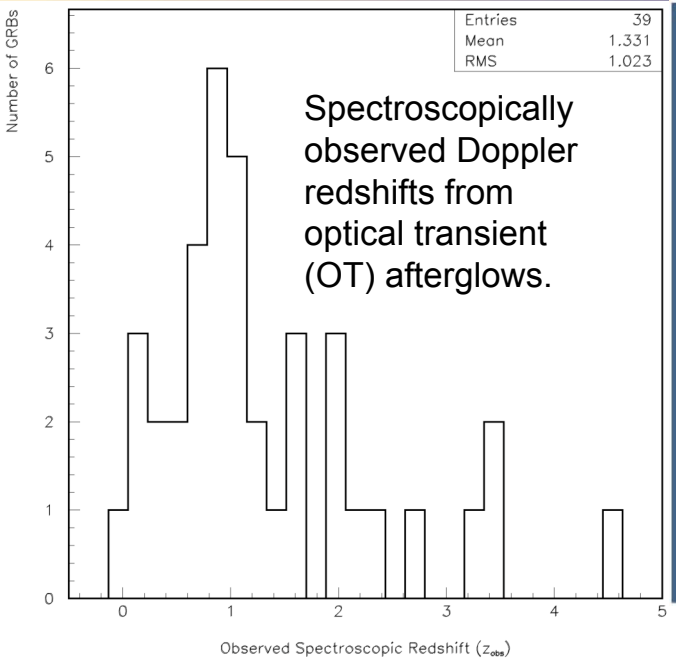

Spectroscopically observed Doppler redshifts from optical transient (OT) afterglows.

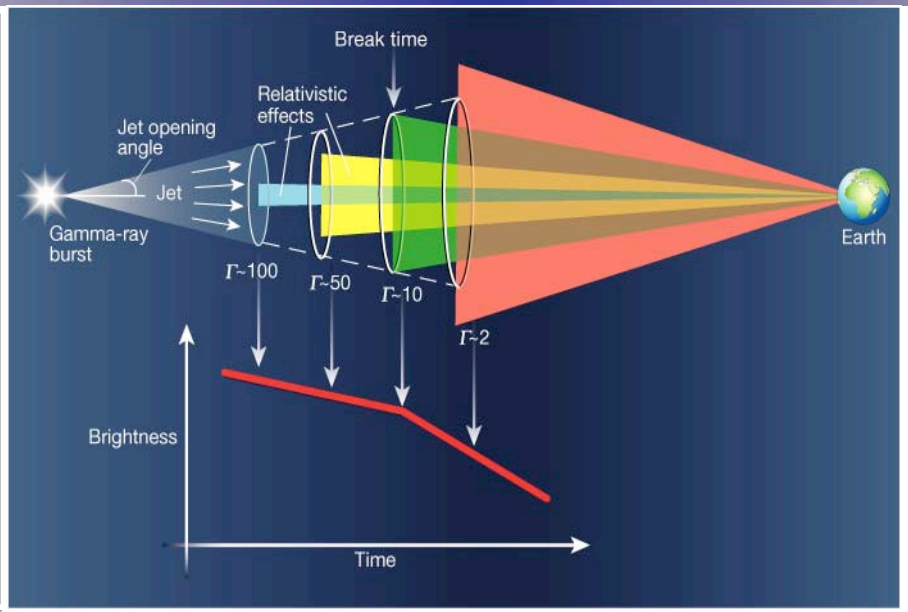

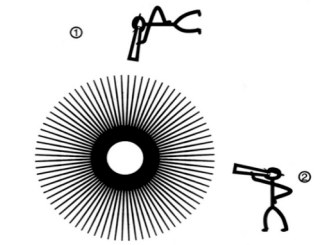

Isotropic Emission

Beamed Emission

Isotropic Emission: ~ 1 GRB/Day → $R_{GRB}^{iso} \sim 0.5$ GRB/(Gpc^3·yr).

Beamed (Jet) Emission: Corrections → $R_{GRB}^{iso} \cdot (4\pi/\Omega_b)$ sr and $E_{iso} \cdot (\Omega_b/4\pi)$ sr. Where: Ω_b = Beaming solid angle (sr)

$$f_b \equiv 1 - \cos\theta_{jet} \equiv \text{Beaming fraction}$$

$$\theta_{jet} \approx 1/\Gamma_{Bulk} \qquad \Gamma_{Bulk} = \frac{1}{\sqrt{1 - v^2/c^2}}$$

GRB030329: Initial Localization & Temporal Spectrum

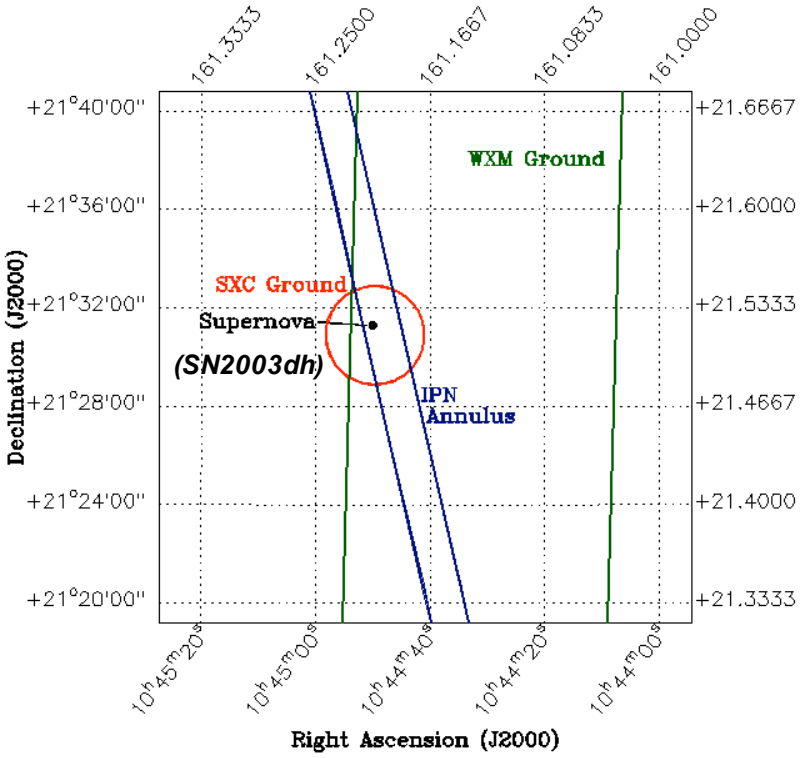

Wide-Field X-ray Monitor (WXM):
2-25 keV, accurate to ≤ 10°.

Soft X-ray Camera (SXC):
0.5-10 keV, accurate to ≤ 0.5°.

French Gamma Telescope (FREGATE): 6-400 keV, 70° FOV

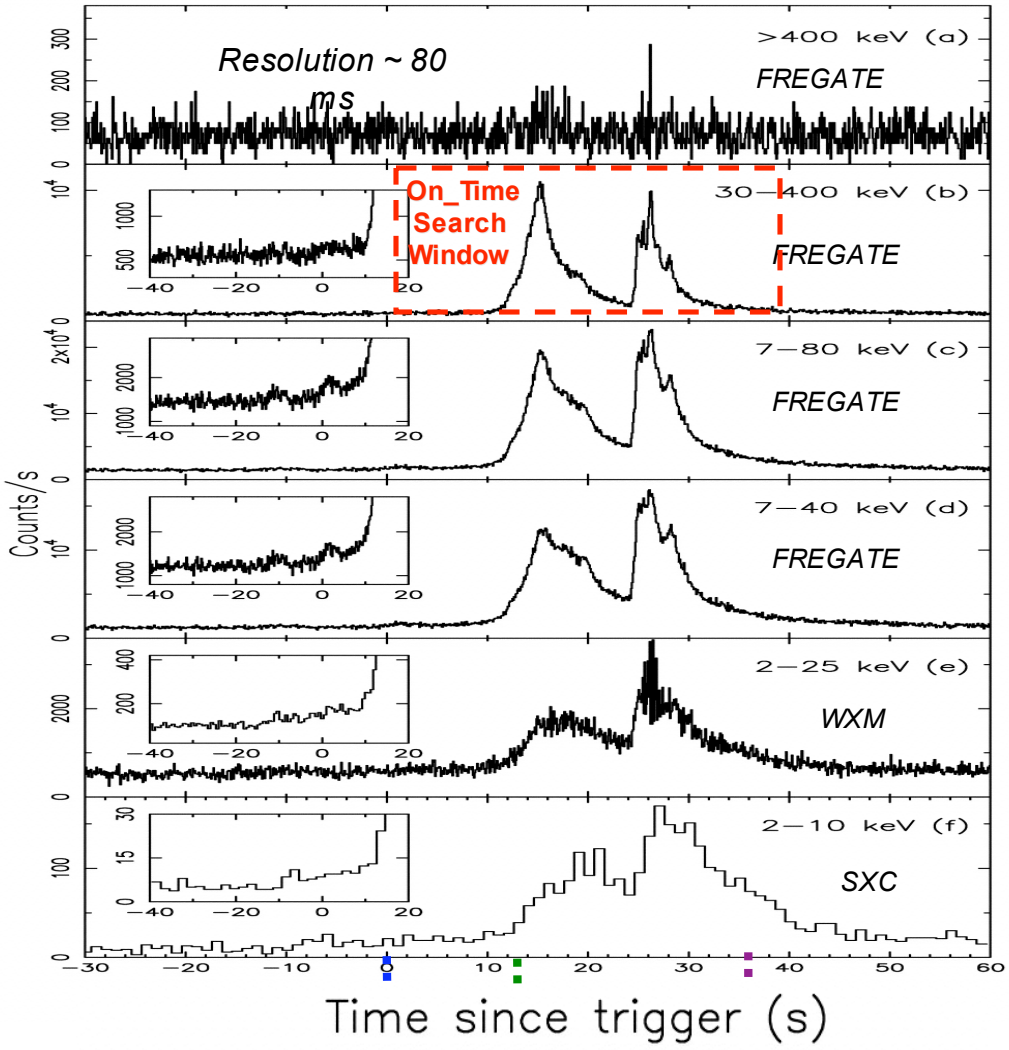

Trigger Time: 41,834.7 UTC^s

30-400 keV Energy Band Pass

T_{90} Time: 22.8 ± 0.5 SI^s

$T_{05} \equiv T_{90}$ Start: +13.01 SI^s

$T_{95} \equiv T_{90}$ End: 41,871.01 UTC^s

Vanderspek, R. et al. ApJ 617, 1251-1257 (2004)

GRB030329: Band Photon Energy Spectrum

- Although the temporal spectra are unique, the energy spectra may be fit an empirical *Band function*, provided the parameters are allowed to vary.

$$N_{\varepsilon_\gamma}(\varepsilon_\gamma) = \begin{cases} A_\gamma \left(\dfrac{\varepsilon_\gamma}{100\text{keV}}\right)^{\alpha} e^{\left(-\frac{\varepsilon_\gamma}{\varepsilon_\gamma^o}\right)} & (\alpha-\beta)\varepsilon_\gamma^o \geq \varepsilon_\gamma \\ A_\gamma \left[\dfrac{(\alpha-\beta)\varepsilon_\gamma^o}{100\,\text{keV}}\right]^{(\alpha-\beta)} e^{(\beta-\alpha)} \left(\dfrac{\varepsilon_\gamma}{100\,\text{keV}}\right)^{\beta} & (\alpha-\beta)\varepsilon_\gamma^o \leq \varepsilon_\gamma \end{cases}$$

Band, D.L. et al. ApJ 413, 281-292 (1993)

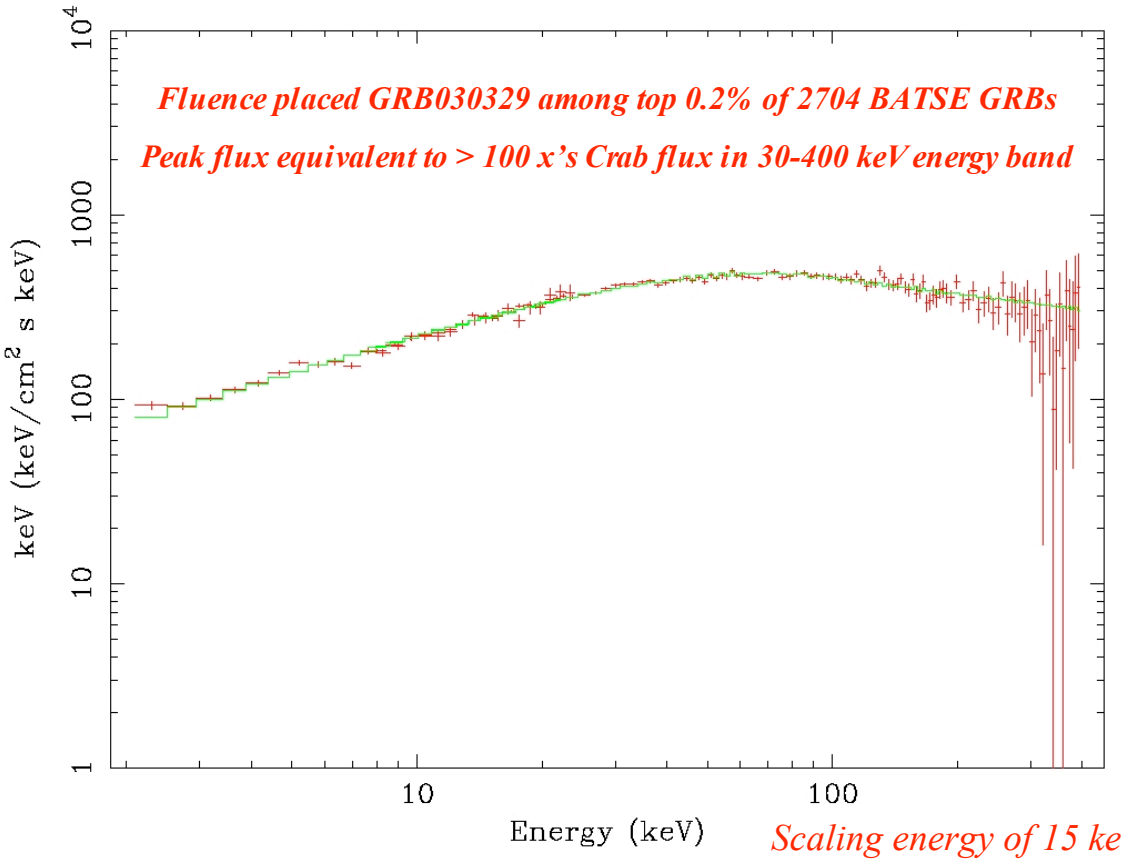

Barraud, C. et al. astro-ph/0311630

Prompt ã - ray emission :

$$\text{Fluence}\,(F_\gamma) = 1.630^{+0.014}_{-0.013} \times 10^{-4}\ \frac{\text{ergs}}{\text{cm}^2}$$

Sakamoto, T. et al. astro-ph/0409128

$$\text{Peak Flux}\,(\Phi_\gamma^{Peak}) \sim 7 \times 10^{-6}\ \frac{\text{ergs}}{\text{cm}^2 \cdot \text{s}}$$

Vanderspek, R. et al. GCN Report 2212

Band Spectral Fit Parameters :

$\alpha = -1.32 \pm 0.02 > -2 \equiv$ Low Index

$\beta = -2.44 \pm 0.08 < -2 \equiv$ High Index

$\varepsilon_\gamma^P = 70.2 \pm 2.3\ \text{keV} \equiv$ Peak Energy

Vanderspek, R. et al. ApJ 617, 1251-1257 (2004)

$$\varepsilon_\gamma^o = \varepsilon_\gamma^P / (2+\alpha) = 103.2 \pm 4.5\ \text{keV}$$

Scaling energy of 15 keV

$$\text{Photon break energy} \equiv \varepsilon_\gamma^b = (\alpha-\beta)\varepsilon_\gamma^o = 115.6 \pm 9.9\ \text{keV}$$

GRB03029: Optical Transient (OT) Afterglow

HETE-II SXC 4' error circle is shown in both plates.

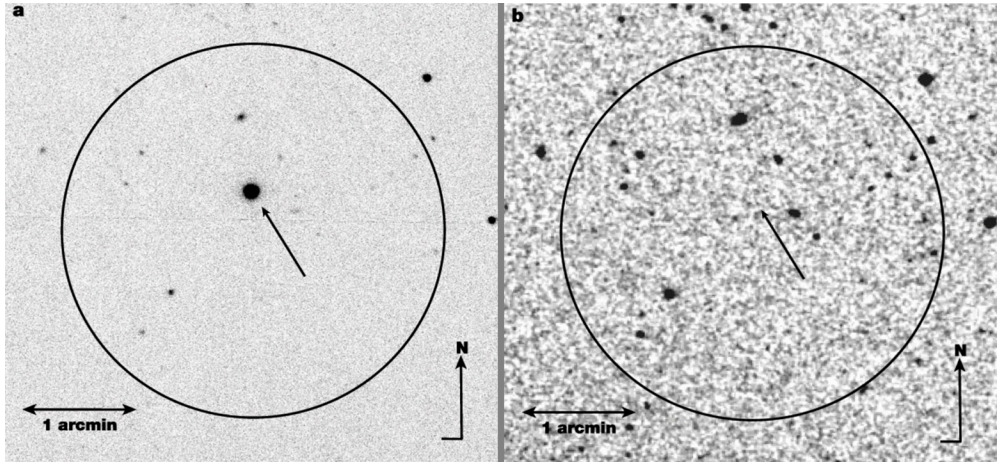

600^s exposure taken on 13^{h}5^m UTC, 29 March 2003 (~1.5^h after prompt g-ray emission).

Comparison with Second Digitized Sky Survey (DSS2) identified 12 magnitude OT.

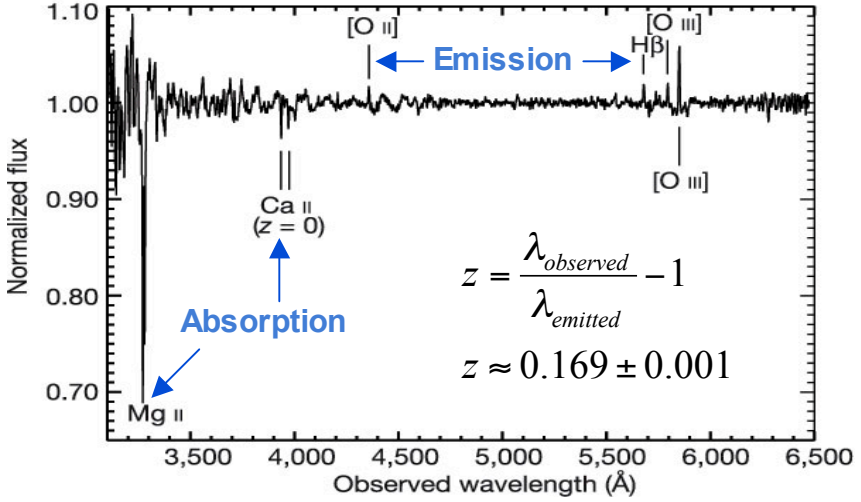

Low Resolution Imaging Spectrometer on Keck I (600^s @ 4.2 Å)

Price, P.A. et al., Nature 423, 844-847 (2003)

$$L_\gamma^{iso} = \Phi_\gamma^{Peak} 4\pi d_L^2,\ \Phi_\gamma^{Peak} \approx 7\times10^{-6}\ \frac{\text{ergs}}{\text{cm}^2\cdot\text{s}}\ \&\ z = 0.168541 \pm 0.000004$$

Bloom, J. et al. GCN Report 2212

$$d_L = \frac{c(1+z)}{H_o}\int_0^z \frac{dz'}{\sqrt{\Omega_\Lambda + \Omega_m (1+z')^3}},\ \Lambda_{CDM} \Rightarrow \left\{\begin{array}{c} H_o = 72 \pm 5\ \frac{\text{km}}{\text{s}\cdot\text{Mpc}} \\ \Omega_M = 0.29 \pm 0.07 \\ \Omega_\Lambda = 0.73 \pm 0.09 \\ z = 0.168541 \pm 0.000004 \end{array}\right\}$$

Spergel et al., ApJS 148, 175-194 (2003)

Redshift + Assumed Cosmological Model → Luminosity distance, which sets the energy scale

$$d_L \approx 2.44^{+0.20}_{-0.18}\times10^{27}\ \text{cm}$$

Close by GRB standards but still cosmological; d_L ~ 2.2 billion light years → Corresponds to Precambrian geologic time, i.e. predates the Earth's first ice age, when Antarctica was located in northern hemisphere!

$$L_\gamma^{iso} \approx 5.24^{+0.86}_{-0.77}\times10^{50}\ \frac{\text{ergs}}{\text{s}}\quad [30\text{-}400\ \text{keV band pass}]$$

Close but Under-luminous

OT Spectral Evolution: GRB2003/SN2003dh

- GRBs/Type Ic SN connection → Collapsar progenitor model.
- Observations consistent with fireball description. Exposed problems with the Cannon Ball model [Dado et al., ApJ 594, L89-L92 (2003)]; as discussed in Taylor et al., ApJ 609 L1-L4 (2004) and Oren et al., MNRAS 353, L35-L40 (2004).

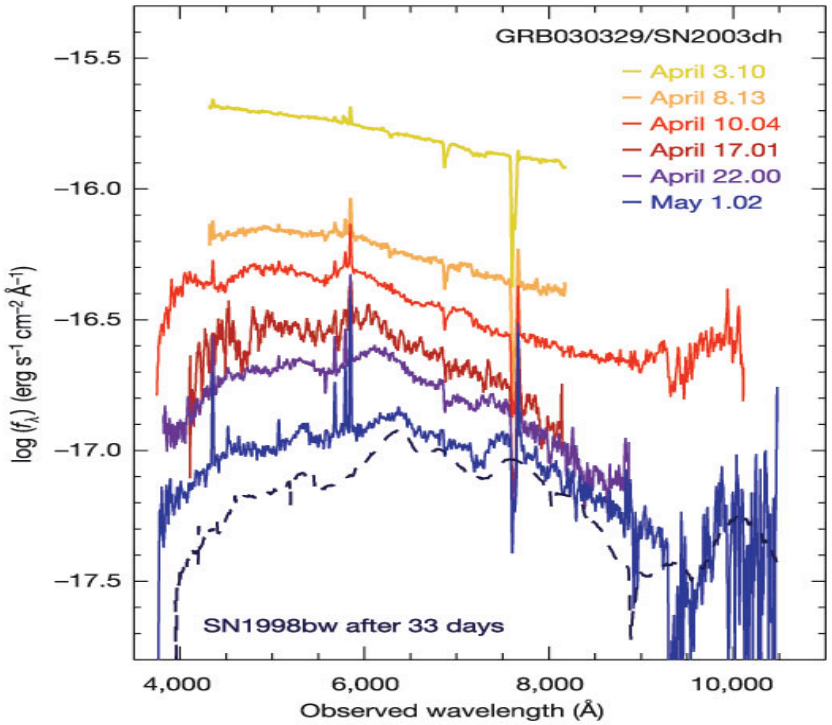

Hjorth et al., Nature 423, 847-850 (2003)

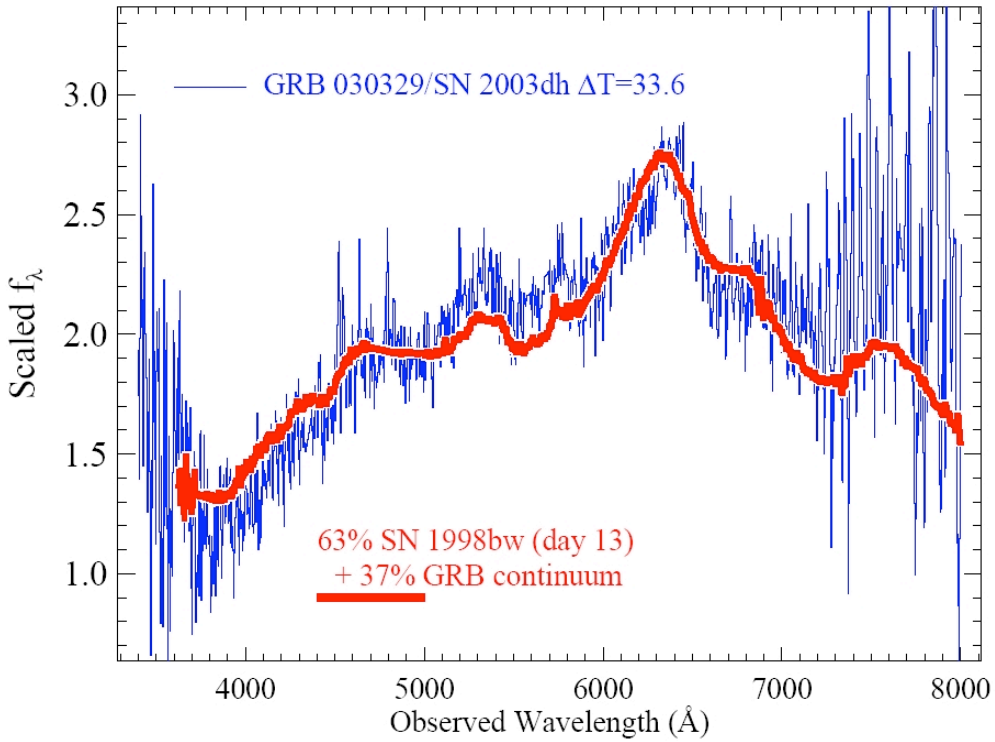

Matheson et al., astro-ph/0307435

GRB030329 Radio Afterglow

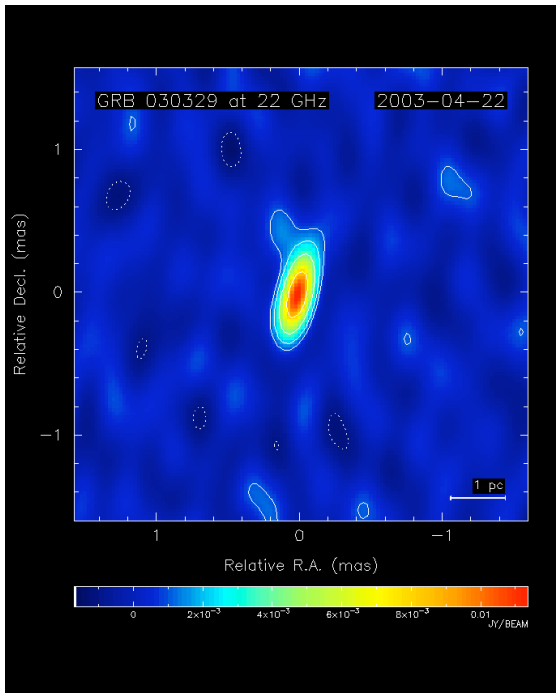

- Radio Counterpart of GRB030329, leads to *mas* positional localization.

$$\alpha_{J2000} = 10^h 44^m 49.^s 9595$$
$$= 161.2081646^\circ$$
$$\delta_{J2000} = +21^\circ 31' 17.''438$$
$$= 21.5215106^\circ$$
$$\pm\sigma_R = 0.''001 = \left(3\times10^{-7}\right)^\circ$$

Taylor et al., GCN Report 2129

- Radio calorimetry revealed break in the afterglow spectrum consistent with collimated prompt emission within a jet of opening half angle $\theta_{jet} \sim 5^\circ \sim 0.09$ rad *[Berger et al., Nature 426, 154-157 (2003)]*. Requires beaming fraction correction:

$$L_\gamma^{jet} = L_\gamma^{iso}\left(1-\cos\theta_{jet}\right) = 1.99^{+0.33}_{-0.29}\times10^{48}\ \frac{\text{ergs}}{\text{s}}$$

- Radio calorimetry provided estimates for fraction of shock energy imparted to the electrons ($\in_e \sim 0.19$) and magnetic field ($\in_B \sim 0.042$) [Frail et al, ApJ 619, 994-998 (2005)].

Leptonic Emission from GRBs?

- Fireball phenomenology predicts MeV-EeV neutrinos in the context of hadronic acceleration.

Regime	ε_ν (eV)	Mechanism/Comments
1	$\sim 10^7$	Collapse/merger of progenitor event (quasi-thermal)
2	$\sim 10^9 - 10^{10}$	Longitudinal decoupling of the baryonic (i.e. n,p) flow in fireball
3	$\sim 10^{12} - \leq 10^{14}$	Precursors $\sim 10-100$ sec before γ_{Prompt} (pp,$p\gamma$ between jet/star)
4	$\sim 10^{14} - 10^{15}$	Photomeson interactions/internal shock, simultaneous* with γ_{Prompt}
5	$\sim 10^{17} - 10^{18}$	Afterglow, $p\gamma$/external (reverse) shock, ~ 10 seconds after γ_{Prompt}

* *Flight time delay due to neutrino mass is negligible for $\varepsilon_\nu \sim PeV$.*

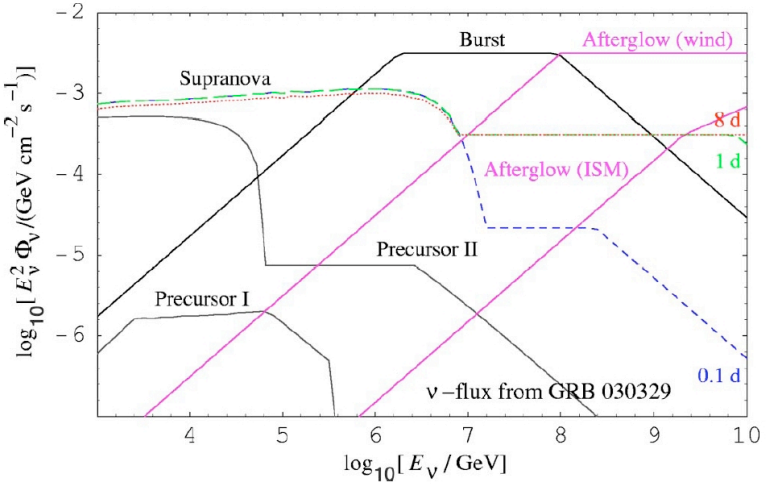

Razzaque, Meszaros & Waxman Phys. Rev. D. 69 023001 (2004)

- Observationally advantageous are TeV-PeV neutrinos – spatial and temporal coincidence with prompt emission results in nearly background free search.
- Original predictions [Waxman & Bahcall, Phys. Rev. D 59 023002], assumed GRBs were CR accelerators and featured averaged BATSE GRB parameters.
- Electromagnetic observables of GRBs are characterized by distributions which span orders of magnitude and differ from burst to burst and class to class.
- Fluctuations may enhance neutrino production [Halzen & Hooper ApJ 527, L93-L96 (1999), Alverez-Muniz, Halzen & Hooper Phys. Rev. D 62, (2000)].
- Positive signal detection is a smoking gun signature of hadronic acceleration – may reveal astrophysical source of CR as well as the microphysics associated with GRBs and intrinsic leptonic properties such as neutrino mass.

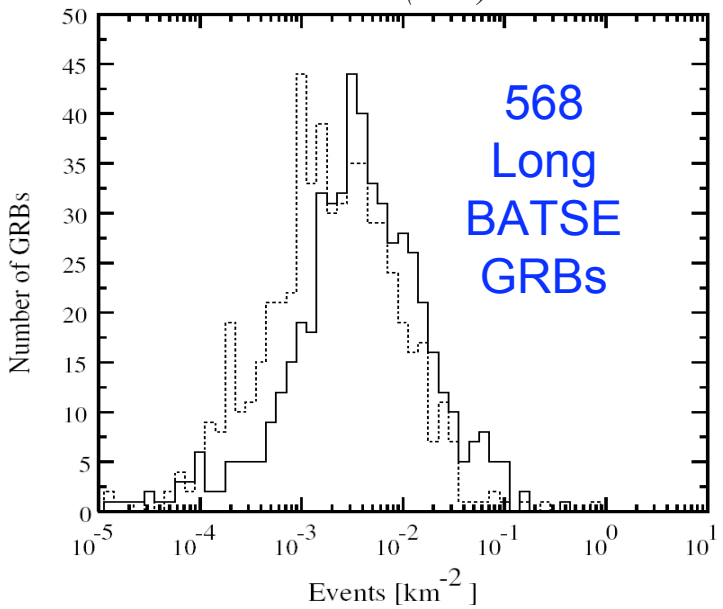

Guetta et al., Astro. Part. 20 (2004) 429-455

The Fireball Phenomenology: GRB-ν Connection

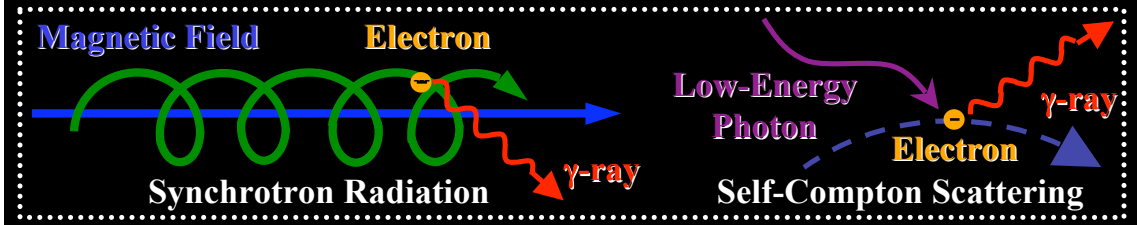

Prompt γ-ray emission of GRB is due to non-thermal processes such as electron synchrotron radiation or self-Compton scattering.

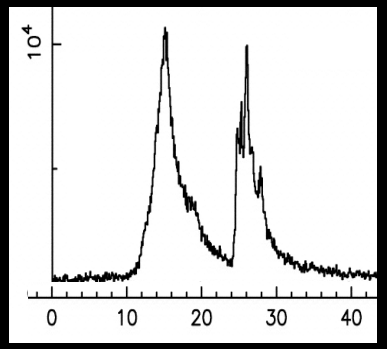

GRB Prompt Emission (Temporal) Light Curve

- Shock variability is a unique "finger-print" reflected in the complexity of the GRB time profile.
- Implies compact object.

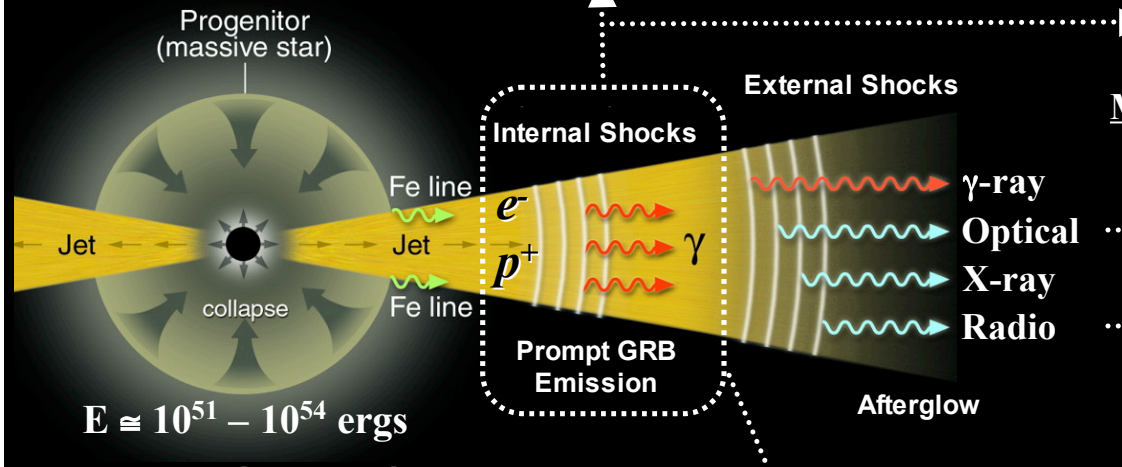

Multi-wavelength Afterglows Span EM Spectrum

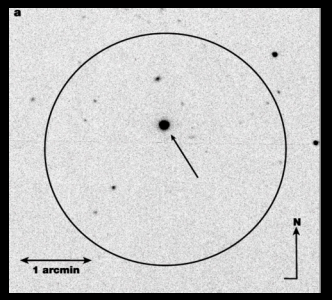

Optical Afterglow

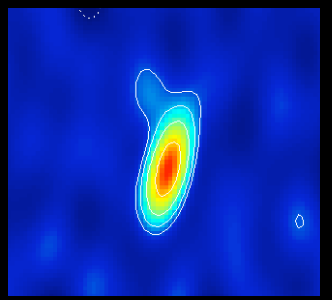

Radio Afterglow

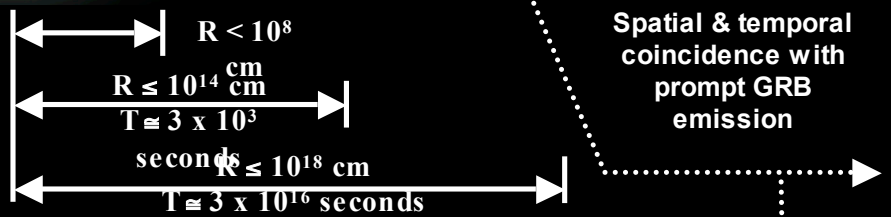

Spatial & temporal coincidence with prompt GRB emission

$E_{cm}^{p\tilde{a}}$ ≡ pã center of mass energy & $E_{\ddot{A}^+}^{Th}$ ≡ Ä⁺ threshold energy.

$$\text{If } E_{cm}^{p\gamma} > E_{\Delta^+}^{Th} \Rightarrow p^+ + \gamma \rightarrow \Delta^+ \rightarrow (n) + \pi^+ \rightarrow \nu_\mu + \mu^+ \rightarrow \nu_\mu + e^+ + \nu_e + \bar{\nu}_\mu$$

Photomeson interactions involving relativistically *(Γ≈ 300)* shock-accelerated protons *($E_p \geq 10^{16}$ eV)* and synchrotron gamma-ray photons *($E_\gamma \approx 250$ keV)* in the fireball wind yield high-energy muonic neutrinos *($E_\nu \approx 10^{14} – 10^{15}$ eV).*

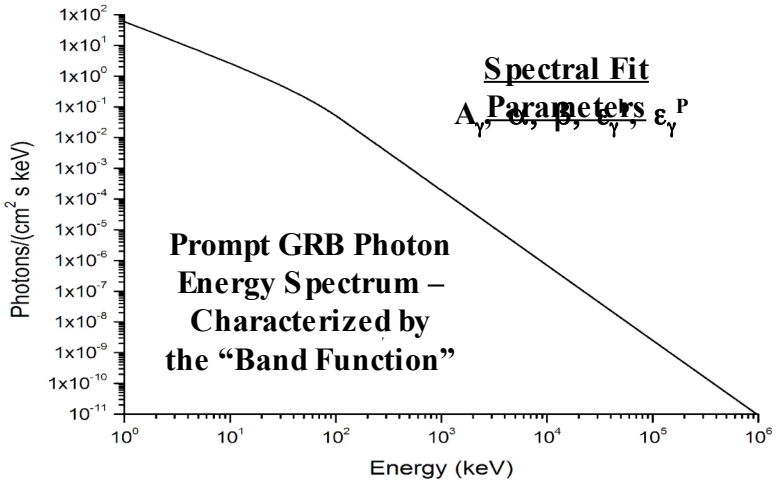

Muon Neutrino Spectrum: Parameterization

$$\varepsilon_{\nu_\mu}^2 \Phi_{\nu_\mu} \approx A_{\nu_\mu} \times \begin{cases} \left(\frac{\varepsilon_{\nu_\mu}}{\varepsilon_\nu^b}\right)^{-\beta-1} & \left(\varepsilon_{\nu_\mu} < \varepsilon_\nu^b\right) \\ \left(\frac{\varepsilon_{\nu_\mu}}{\varepsilon_\nu^b}\right)^{-\alpha-1} & \left(\varepsilon_\nu^b < \varepsilon_{\nu_\mu} < \varepsilon_\pi^b\right) \\ \left(\frac{\varepsilon_{\nu_\mu}}{\varepsilon_\nu^b}\right)^{-\alpha-1}\left(\frac{\varepsilon_{\nu_\mu}}{\varepsilon_\pi^b}\right)^{-2} & \left(\varepsilon_{\nu_\mu} > \varepsilon_\pi^b\right) \end{cases}$$

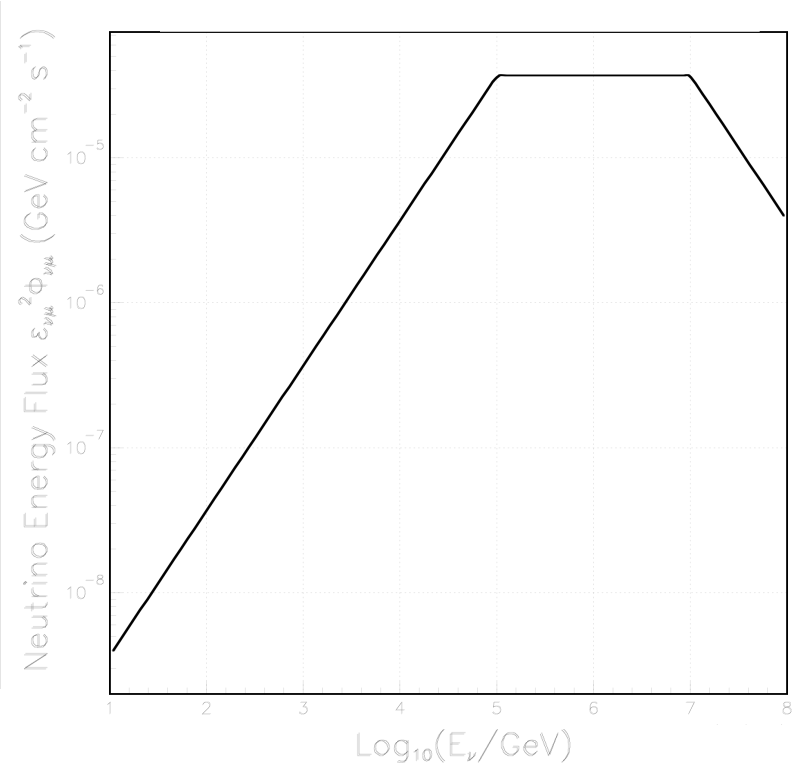

$$A_{\nu_\mu} \approx \frac{F_\gamma f_\pi}{8 \in_e \ln(10) \Gamma_{90}} \equiv \text{Normalization}$$

$$f_\pi \cong 0.2 \times \frac{L_{\tilde{a},52}}{\Gamma_{2.5}^4 t_{v,-2} \varepsilon_{\tilde{a},\mathrm{MeV}}^b (1+z)} \equiv \text{Proton effeciency}$$

$$\Gamma \geq\sim 276 \left[L_{\tilde{a},52}\, t_{v,-2}^{-1}\, \varepsilon_{\tilde{a},\mathrm{MeV}}^{\max} (1+z)\right]^{1/6} \equiv \text{Bulk Lorentz Boost Factor}$$

$$\varepsilon_\nu^b \approx \left[\frac{7\times10^5}{(1+z)^2} \frac{\Gamma_{2.5}^2}{\varepsilon_{\tilde{a},\mathrm{MeV}}^b}\right] \mathrm{GeV} \equiv \text{Neutrino break energy}$$

Neutrino spectrum is expected to trace the photon spectru $\varepsilon_{\nu_\mu} \propto \varepsilon_p \propto \varepsilon_\gamma^{-1}$

$$\varepsilon_\pi^b \approx \left[\frac{10^8}{(1+z)} \in_e^{1/2} \in_B^{-1/2} (L_{\tilde{a},52})^{-1/2} \Gamma_{2.5}^4\, t_{v,-2}\right] \mathrm{GeV} \equiv \text{Synchrotron break energy}$$

$$L_{\gamma,52} \equiv \frac{L_\gamma}{10^{52}\ \mathrm{ergs/s}}$$

$$\Gamma_{2.5} \equiv \frac{\Gamma}{10^{2.5}}$$

$$t_{v,-2} \equiv \frac{t_v}{10^{-2}\ \mathrm{s}}$$

$$\varepsilon_{\tilde{a},\mathrm{MeV}}^b \equiv \frac{\varepsilon_\gamma^b}{1\,\mathrm{MeV}}$$

$$\varepsilon_{\tilde{a},\mathrm{MeV}}^{\max} \equiv \frac{\varepsilon_\gamma}{100\ \mathrm{MeV}}$$

Stamatikos, Band, Hooper & Halzen (In preparation)

Guetta et al., Astroparticle Physics 20, 429-455 (2004)

Neutrino Flux Models for GRB030329

Model	Model 1	Model 2	Model 3
Parameter	Discrete Isotropic	Discrete Jet	Average Isotropic
Fluence [F_γ] (ergs/cm^2)	(1.63 ± 0.014) x 10^{-4}	(1.63 ±0.014) x 10^{-4}	6.00 x 10^{-6}
Peak Flux [Φ_γ] (ergs/cm^2/s)	~7 x 10^{-6}	~7 x 10^{-6}	2 x 10^{-6}
Redshift [z]	0.168541 ± 0.000004	0.168541 ± 0.000004	1
Low Spectral Index [α]	-1.32 ± 0.02	-1.32 ± 0.02	-1
High Spectral Index [β]	-2.44 ± 0.08	-2.44 ± 0.08	-2
Peak Energy [ε_γ^p] (keV)	70.2 ± 2.3	70.2 ± 2.3	1000
Break Energy [ε_γ^b] (keV)	115.6 ± 9.9	115.6 ± 9.9	1000
Luminosity [L_γ] (ergs/s)	(5.24 ± 0.82) x 10^{50}	(1.99 ± 0.31) x 10^{48}	1 x 10^{52}
Bulk Lorentz Boost [Γ]	178	70	300
Proton Efficiency [f_π]	0.77	0.12	0.2
Normalization [$A_{\nu\mu}$] (GeV/cm^2/s)	9.86 x 10^{-4}	1.54 x 10^{-4}	8.93 x 10^{-6}
Neutrino Break Energy [ε_ν^b] (GeV)	1.404951 x 10^6	2.19343 x 10^5	1 x 10^5
Synchrotron Break Energy [ε_π^b] (GeV)	7.9832941 x 10^7	3.1543774 x 10^7	1 x 10^7

Stamatikos for the IceCube Collaboration, Kurtzweil and Clarke, Proceedings of 29th ICRC 2005

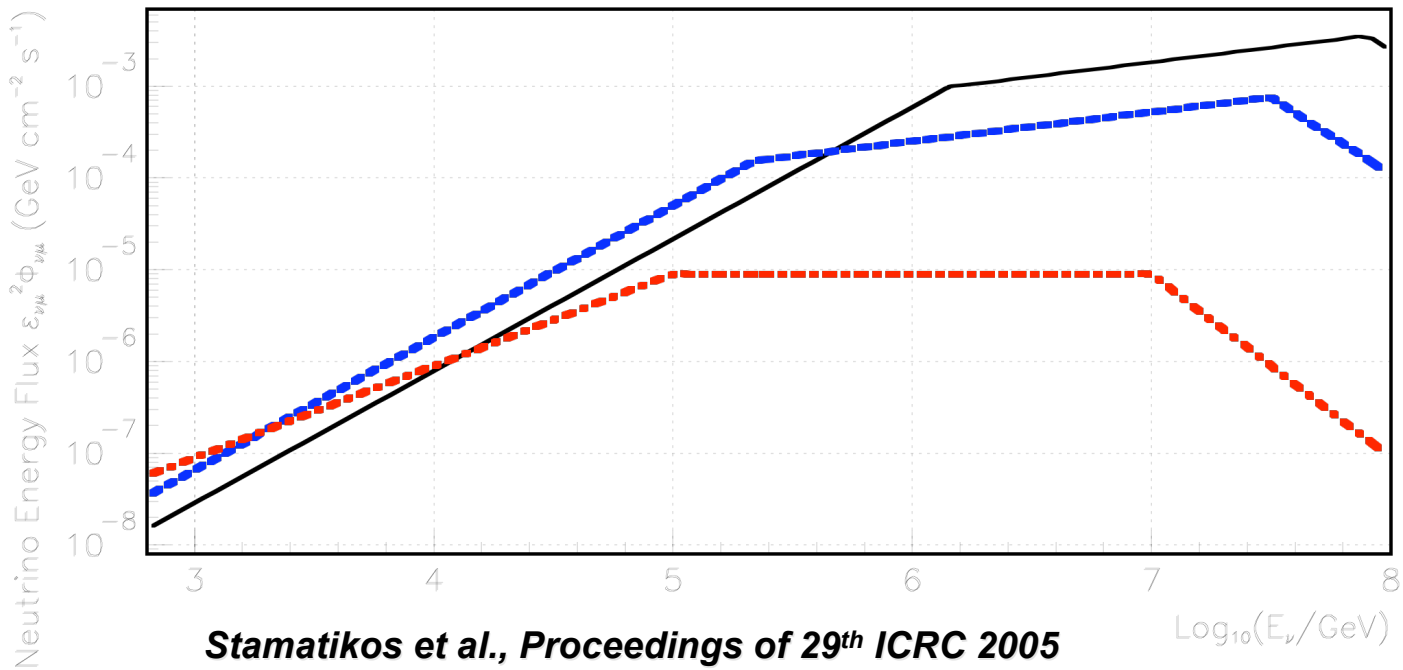

Stamatikos et al., Proceedings of 29th ICRC 2005

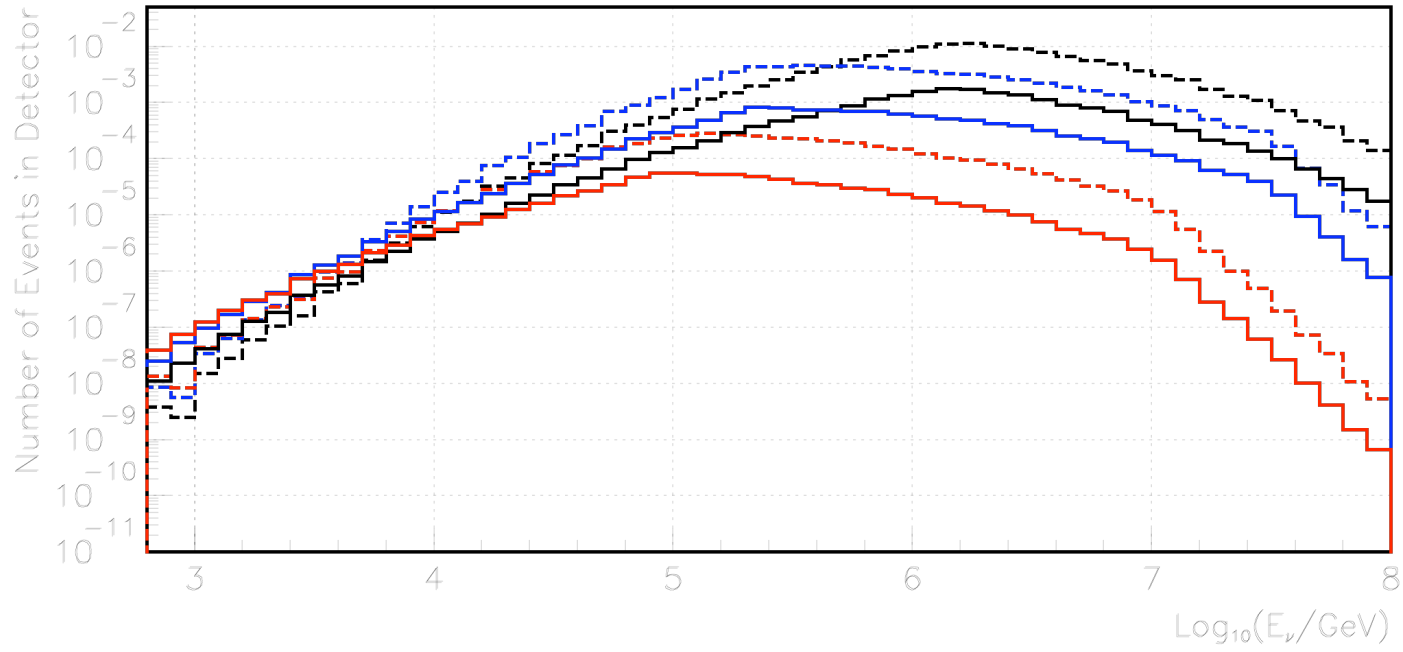

Order of magnitude differences in mean energy and number of events in detector.

Neutrino Flux Models

Model 1: Discrete Isotropic

Model 2: Discrete Jet

Model 3: Average Isotropic

$$\varepsilon_\nu^b = \left[\frac{7\times10^5}{(1+z)^2}\frac{\Gamma_{2.5}^2}{\varepsilon_{\tilde{a},\mathrm{MeV}}^b}\right] \mathrm{GeV}$$

Up-going Events, Detected via charged current interactions:

$$\nu_\mu + N \rightarrow \mu^\pm + X$$

IceCube (Dashed)

Model 1: Discrete Isotropic (0.1308 events)

Model 2: Discrete Jet (0.0691 events)

Model 3: Average Isotropic (0.0038 events)

AMANDA-II (Solid)

Model 1: Discrete Isotropic (0.0202 events)

Model 2: Discrete Jet (0.0116 events)

Model 3: Average Isotropic (0.0008 events)

Statistical Blindness & Unbiased Analysis

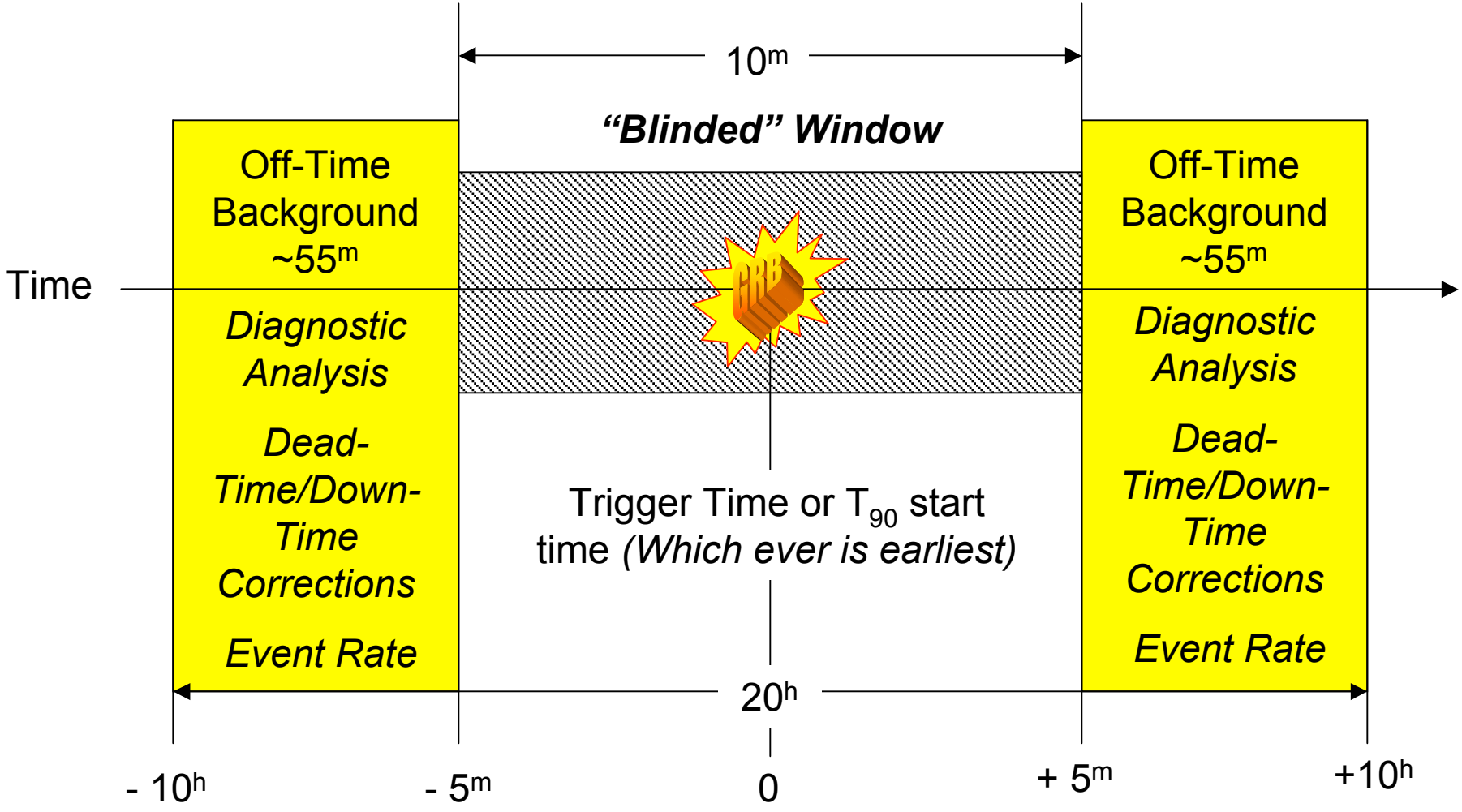

Nominal Extraction: 2^h
Nominal Off-Time Interval: 110^m

→ Systematic dead-time
Down-time of detector

→ True Off-time
Bkgd Event rate

Event Quality Selection: Optimization

- Multiple observables investigated → single, robust criterion emerged - maximum size of the search bin radius (Ψ), i.e. the space angle between the reconstructed muon trajectory (θ_μ, φ_μ) and the positional localization of the GRB (θ_{GRB}, φ_{GRB}) :

$$\cos\Psi \equiv \sin\theta_\mu \sin\theta_{GRB} \cos\left(\phi_\mu - \phi_{GRB}\right) + \cos\theta_\mu \cos\theta_{GRB}$$

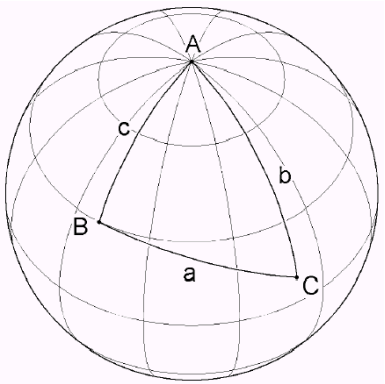

Fundamental formula of spherical trigonometry

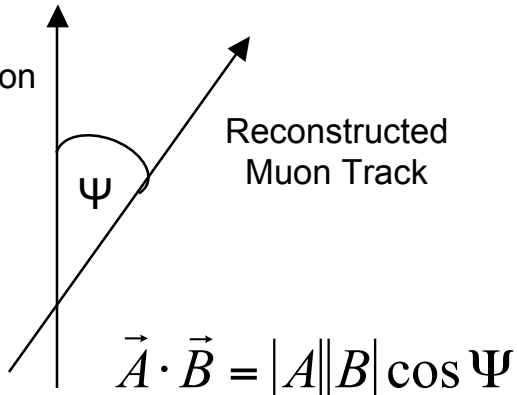

$$\vec{A}\cdot\vec{B} = \left|A\right|\left|B\right|\cos\Psi$$

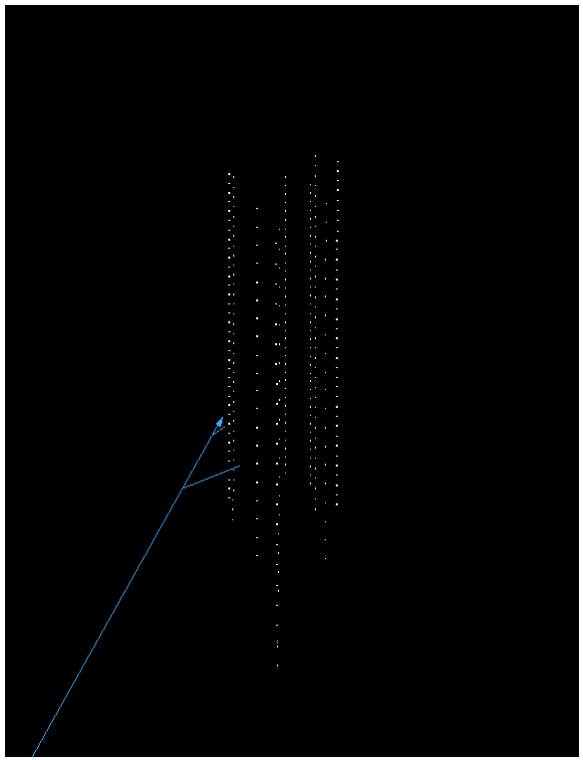

- Up-going events topologically identified via maximum likelihood method.
- Method A: Best limit setting potential – Model Rejection Potential (MRP)
  Method → achieved via minimization of the model rejection factor (MRF): $MRF \equiv \frac{\mu_{90}}{n_s}$

  Hill & Rawlins Astropart. Phys. 19, 393-402 (2003), Feldman & Cousins Phys. Rev. D 57, 3873-3889 (1998)
- Method B: Discovery potential – Model Discovery Potential (MDP)
  Method → achieved via minimization of the model discovery factor (MDF): $MDF \equiv \frac{\mu'_{90}}{n_s}$

  Hill, Hodges & Stamatikos (in preparation)

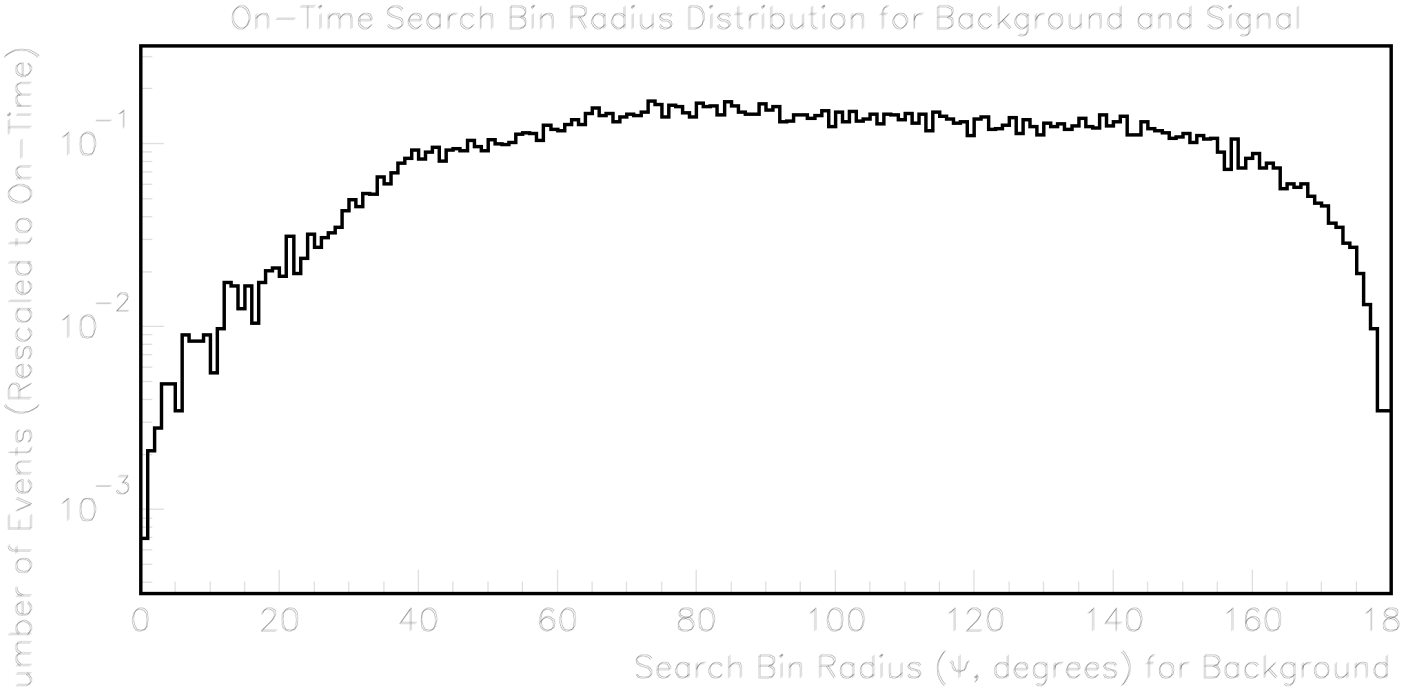

Off-Time Background

24,972 ± 158 Events in 57,328.04 seconds. Expected background rate: 0.436 ± 0.003 Hz

Renormalized to search window duration (40/57,328.04).

$n_b = 17.44 \pm 0.012$

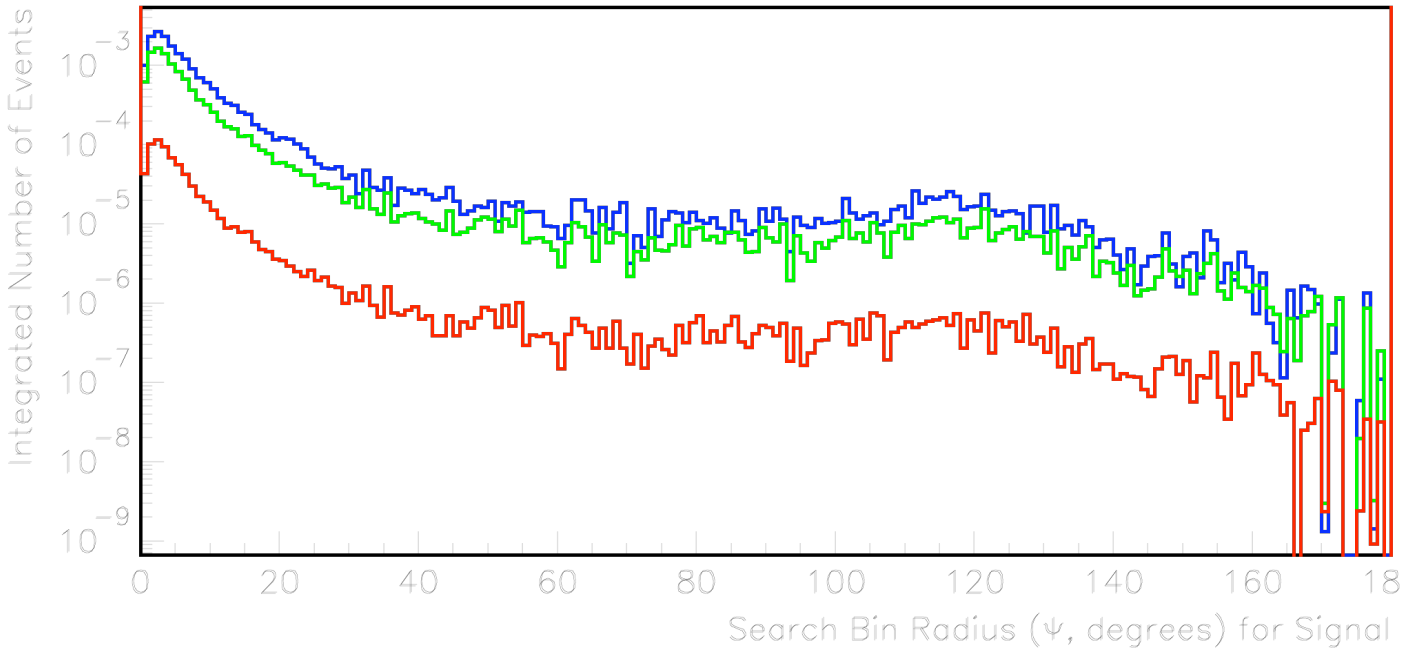

On-Time Signal

Blue – Model 1

0.0202 Events

Green – Model 2

0.0116 Events

Red – Model 3

0.0008 Events

40 Seconds

Signal Sensitivity as a Function of Search Bin Radius for Model 1

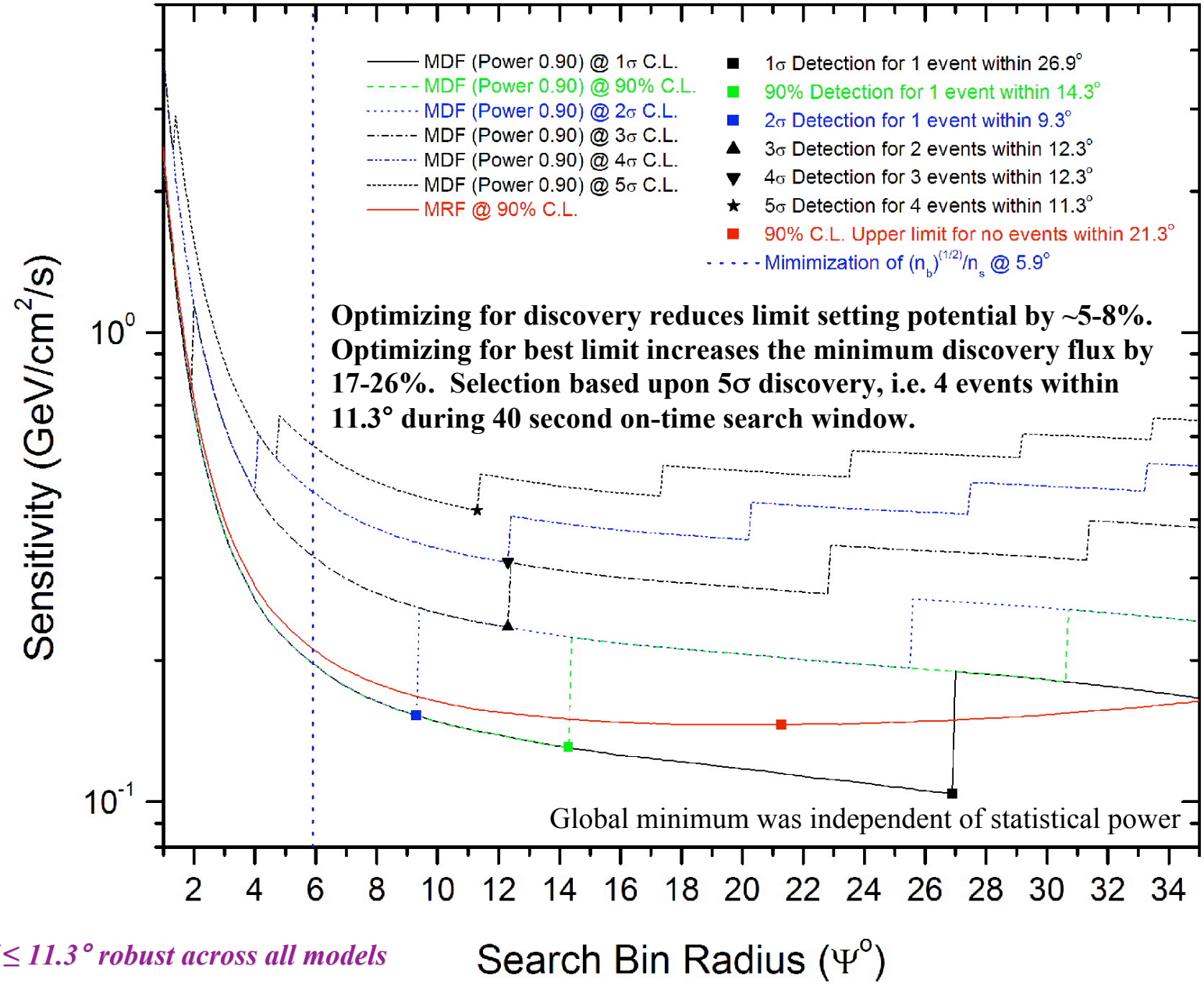

Ψ ≤ 11.3° robust across all models

MDF = Model Discovery Factor (Optimized for Detection)

MRF = Model Rejection Factor (Optimized for Best Upper Limit)

Signal Efficiency & Background Rejection

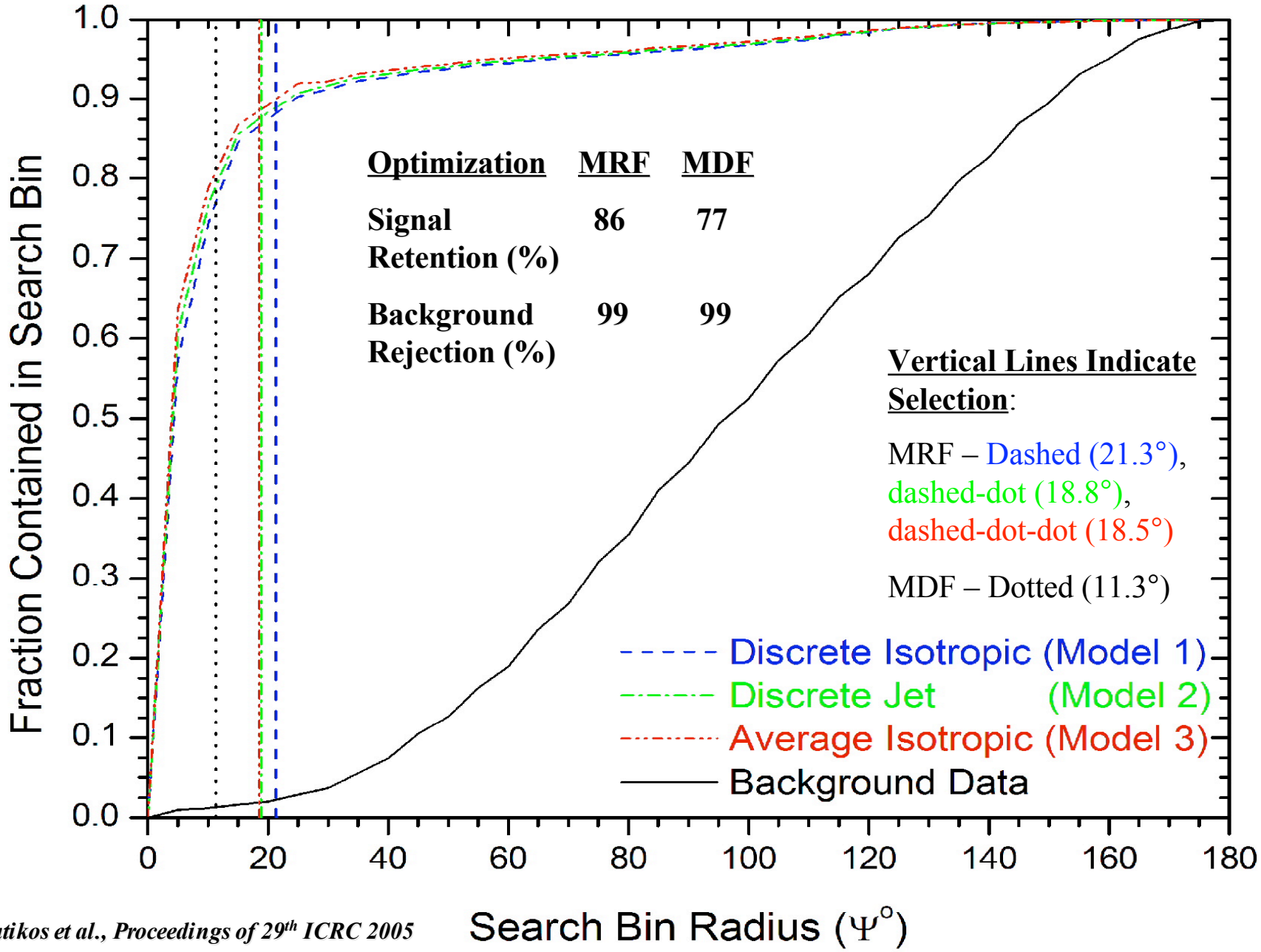

Stamatikos et al., Proceedings of 29th ICRC 2005

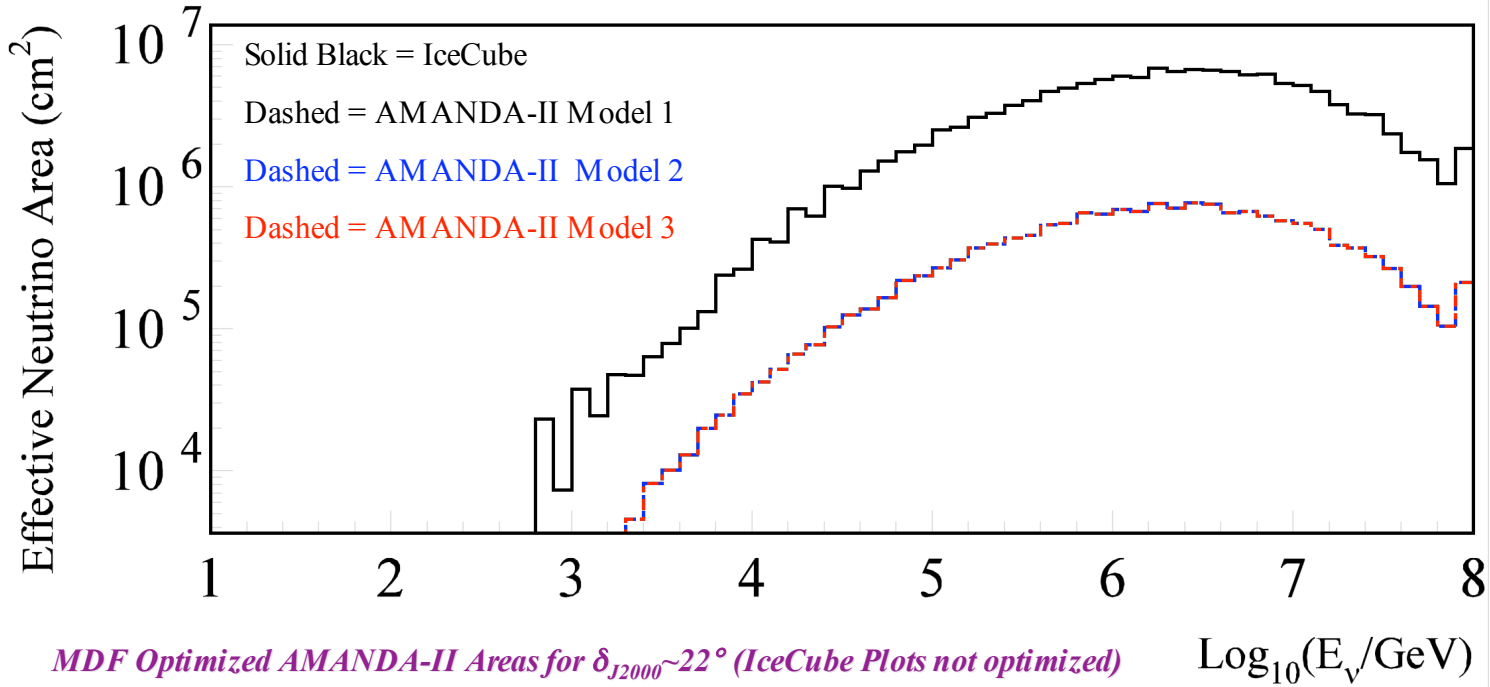

MDF Optimized AMANDA-II Areas for δ_{J2000}~22° (IceCube Plots not optimized)

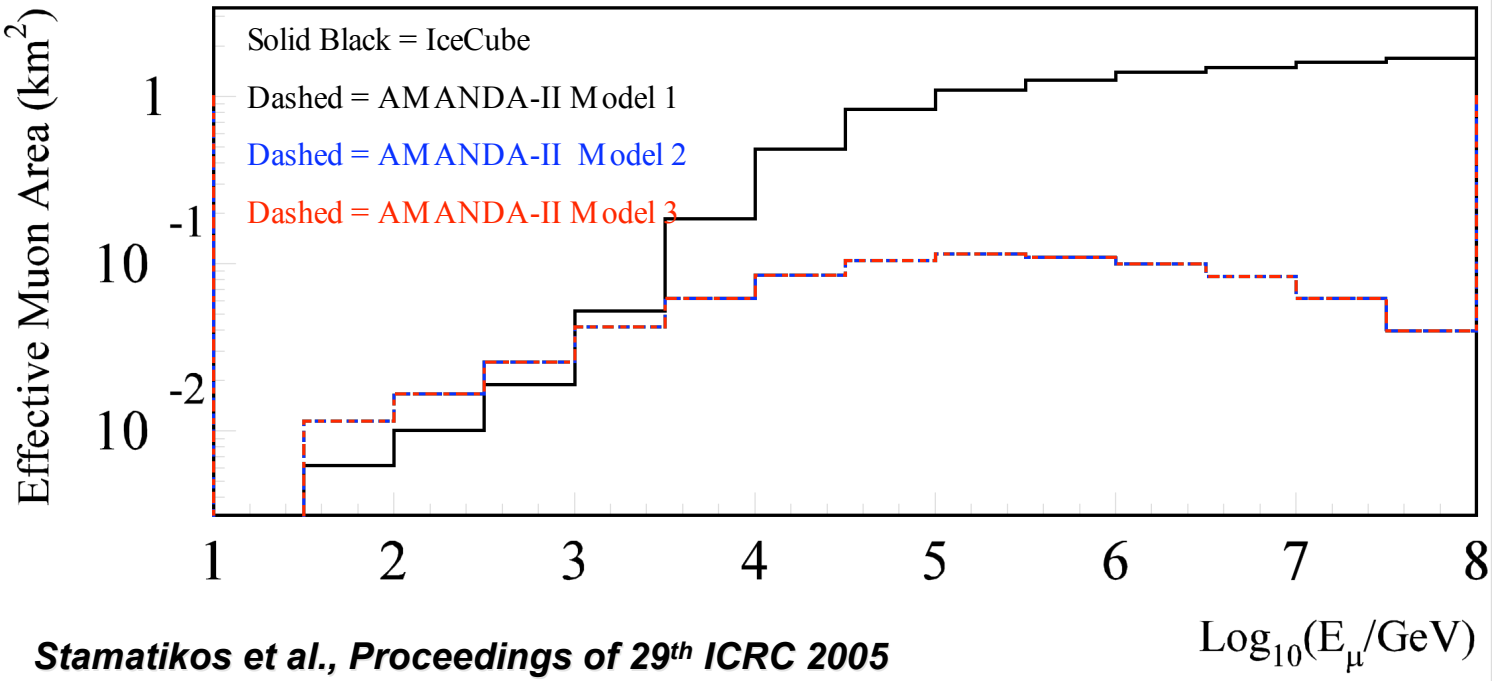

Stamatikos et al., Proceedings of 29th ICRC 2005

Muon neutrino effective area:

AMANDA-II:
~ 80 m^2 @
~2 PeV

IceCube:
~700 m^2 @
~2 PeV

Muon effective area for energy at closest approach to the detector:

AMANDA-II:

~100,000 m^2 @
~200 TeV

IceCube:

~ 1 km^2 @
~200 TeV

Summary of Preliminary Results: GRB030329

Flux Model	Maximum Search Bin Radius		Expected Number of Background Events			Expected Number of Signal Events			Observed Number of Events		Optimization Method		GeV/cm^2/s	
	Ψ^A (°)	Ψ^B (°)	n_b	$n_b^{A'}$	$n_b^{B'}$	N_s	n_s	$n_s^{B'}$	n_{obs}	n_{obs}^B	MRF (A)	MDF (B)	Sensitivity^B	Limit^B
1	21.3	11.3	17.44	0.23	0.06	0.1308	0.0202	0.0156	15	0	152	424	0.157	0.150
2	18.8	11.3	17.44	0.17	0.06	0.0691	0.0116	0.0092	15	0	256	716	0.041	0.039
3	18.5	11.3	17.44	0.17	0.06	0.0038	0.0008	0.0006	15	0	3864	10794	0.036	0.035

Primed variables indicate value after selection. Superscripts indicate A=MRF and B=MDF optimization method.

Results consistent with null signal, and do constrain the models tested in AMANDA-II.

Comparison with Other Authors

1. The number of expected events in IceCube (N_s) for model 1 is consistent with *Razzaque, Meszaros & Waxman Phys. Rev. D. 69 023001 (2004),* when neutrino oscillations are considered.
2. The number of expected events in IceCube (N_s) for model 3 is consistent with *Guetta et al, Astropart. Phys. 20, 429-455 (2004).*
3. The number of expected events in IceCube (N_s) for model 3 is consistent with *Ahrens et al., Astropart. Phys. 20, 507-532 (2004)* when the assumptions of *Waxman & Bahcall, Phys. Rev. D 59, 023002 (1999)* are considered.

Conclusions & Future Outlook

1. Leptonic signatures from GRBs would be a smoking gun signal for hadronic acceleration; revealing a possible acceleration mechanism for high energy CRs as well as insight to the microphysics of the burst.
2. TeV-PeV neutrinos are observationally advantageous since correlative constraints lead to nearly background free searches.
3. Correlative leptonic observations of discrete GRBs should utilize the electromagnetic observables associated with each burst.
4. Although the event quality selection was robust across all models tested, observed variance in detector response unequivocally demonstrates the value of discrete modeling, especially in the context of astrophysical constraints on models for null results.
5. New era of sensitivity with Swift and IceCube – more complete electromagnetic descriptions of GRBs, e.g. redshift, beaming, etc. When not available, estimator methods exist for redshift and jet angle.
6. Similar results have been demonstrated in the context of a diffuse ensemble of GRBs [Becker, Stamatikos, Halzen, Rhode (submitted to Astroparticle Physics)].

Synergy of Gamma-Ray & Neutrino Astronomy!

Swift
2004

GLAST
2007

AMANDA
Since 1997

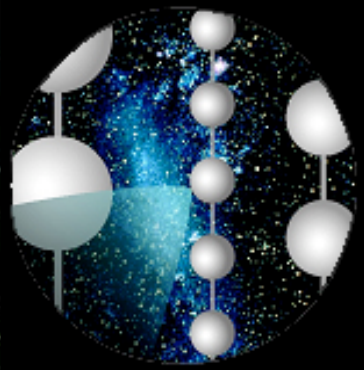

IceCube
2005 - 2010